2020-32-2313

Wall Heat Flux on Impinging Diesel Spray Flame: Effect of Hole size and Rail Pressure at Similar Injection Rate Condition

Rizal Mahmud[1,2], Toru Kurisu[2], Nasrul Ilminnafik[3], Keiya Nishida[2], and Yoichi Ogata[2].
[1]Institute Technology Adhi Tama Surabaya, [2]University of Hiroshima, [3]University of Jember

Abstract

The fuel economy of recent small size DI diesel engines has become more and more efficient. However, heat loss is still one of the major factors contributing to a substantial amount of energy loss in engines. In order to a full understanding of the heat loss mechanism from combustion gas to cylinder wall, the effect of hole size and rail pressure at similar injection rate condition on transient heat flux to the wall were investigated. Using a constant volume vessel with a fixed impingement wall, the study measured the surface heat flux of the wall at the locations of spray flame impingement using three thin-film thermocouple heat-flux sensors. The results showed that the transferred heat was similar under similar injection rate profiles. However, in case of flame luminosity, temperature distribution, characteristic of local heat flux and soot distribution was also similar except the smaller nozzle hole size with higher injection pressure. Moreover, we confirmed that the relation between *Nusselt number* and *Reynolds number* is a useful measure for describing the heat transfer phenomena in diesel combustion.

Introduction

In Direct-Injection (DI) Diesel engine, fuel spray characteristics is the most significance factor which has an effect on the fuel-air mixture formation process, flame development and emissions. Likewise, these possibilities offered by diesel spray such as nozzle hole area and injection pressure became important considerations when combustible fuel-air mixture formation takes place in combustion chamber. Therefore, more fully controlling the mixture formation of the spray is one of the key techniques in further improvements regarding spray combustion process that determines engine performance and emissions.

Fuel injection rate profile can be identified as fuel spray characteristics with temporal change of injection rate during the injection period. This injection rate profile depends on nozzle hole characteristics (size, number of holes, etc.), injection strategies (split injection, injection pressure, etc.) and fuel properties (volume, type, etc.). Some researchers [1,2,3,4] have done conducted the injection strategy based on the injection rate profile. For example, Wakisaka and Azetsu [1,2] used triangular injection rate profile with different slopes of injection rates rise and fall to observe spray combustion and emission formation. It was found that the injection rate profile affected the temporal change of spray evolution, flame temperature and emission. Furthermore, this injection rate profile affected the regions of soot production.

The injection strategy based on the injection rate profile to observe the mixture formation and combustion was explored by Yang et al. [4] The injection rate profile was performed by both with and without pre-injection. It was shown that the vapor distribution of split injection was much more homogeneous than that of the single one. However, the second main injection caught up with the previous injection's flame, which deteriorated the combustion then resulted in higher soot generation.

As described by the previous studies mentioned above, the injection rate profile was found to have significant effect on mixture formation, combustion and emissions. As a result, thanks to the injection strategy improvement and advanced emission control technologies, modern small-size DI diesel engines have become more efficient in fuel economy and produced low emissions recently. However, heat loss is still one of the major factors that contributes to substantial amount of energy loss for engines. Therefore, a thorough understanding of the heat loss mechanism from combustion gas to the cylinder wall would be necessary to maximize thermal efficiency in the design of future engines.

In order to achieve better thermal efficiency of the small diesel engine, it is important to understand and clarify correlations between injection rate profile and heat transfer. For this reason, this paper mainly focuses to investigate the mechanism of heat transfer on various of nozzle hole size and injection pressure under similar injection rate profile. Additionally, this research also attempts to investigate the heat transfer coefficient and heat transfer correlation (relation between *Nusselt number* and *Reynolds number*) to understand the effect of flow induced by the spray flame.

Experimental Set-Up and Procedures

Constant Volume Vessel

The experiment was conducted using high-pressure and high-temperature constant volume vessel, as shown in Figure 1. The set-up we used can be found in the previous report [5]. There were four side windows to it. Two of them have been installed for visualization with transparent quartz windows. The others were provided for an injector and a spray impingement flat wall plate facing each other.

The impinging distance between the nozzle tip to the wall was set at 40 mm. Three K-type thermocouples were mounted near the wall, and the remaining one was installed under the nozzle tip at a distance of 5 mm, which was positioned between the tip of the nozzle and the wall. Diesel fuel was injected into the chamber when the ambient temperature was reached at the target temperature determined by thermocouple mounted in the middle of nozzle tip and wall. It should be noted that the temperature difference of thermocouples became within 5K. Injection pulse values were defined by the injection rate in advance.

High-Speed Video Camera Observation

Spray flame behavior was obtained from a high-speed camera (Nac Image Technology Inc, HX-3). Figure 1(b) presents the optical set-up of high-speed video camera observation and its arrangement. A high-speed color video camera was operated with following setting: the camera resolution of 320 x 448 pixels and an image acquisition rate of 20,000 frame per second (fps). Mie scattering method was adopted to support the spray impingement illumination photography.

The two-color method was applied to the luminous flame in order to find the relation between diesel flame and wall heat loss. Two-color method was used for observing the line of sight of soot concentration and local temperature distribution. As reported in Ahn, at al. [6] the principle of the two-color method utilizes radiation intensity from soot particles through the combustion process in order to calculate the flame temperature. A standard light illuminant was used for the calibration of the two-color method.

Heat Flux Measurement

Three Alumel/Chromel Thin Film Thermocouple Heat Flux (TFTHF) sensors (Medtherm 10702B) shown in Figure 1 have been mounted on the impingement surface side of the wall to measure local heat flux distribution. The sensor consists of two thermocouple sensors. One of them is a surface temperature sensor and the other one is an inner temperature sensor. Its diameter is ø 1.55mm, and distances between thermal contacts (surface and inside) is 3.30mm.

The distance of thin film thermocouple heat flux sensor between each TFTHF sensor is 10 mm as shown in Figure 1 (a). Positions of three TFTHF sensors are designated as Position1 (center of wall impingement), Position2 and Position3, respectively. The equation employed for instantaneous local heat flux and total heat loss can be found in our previous report [5].

Whenever the experimental condition changes, we cleaned the wall surface, as built-up wall deposits from the combustion process affect the measurement accuracy, which has also been reported by to Woschni and Huber [7].

Furthermore, apart from importance of total heat loss from combustion gas to the cylinder wall, understanding the mechanism of heat transfer coefficient (h) is also important to know. Steady state heat transfer coefficient is expressed in equation (1), but this relation is also applicable to the transient heat transfer. q_{wall} is transient local heat flux and T_{wall} is instantaneous local temperature, both of which are obtained from TFTHF sensors measurement. T_g is gas temperature in combustion chamber.

$$h = \frac{q_{wall}}{T_g - T_{wall}} \quad (1)$$

Gas temperature during combustion varies both spatially and temporally and it is difficult to determine adequate value. There exists large temperature gradient distributed in flame according to previous study [8]. Then we used local temperature near wall which was obtained from two-color method analysis as gas temperature.

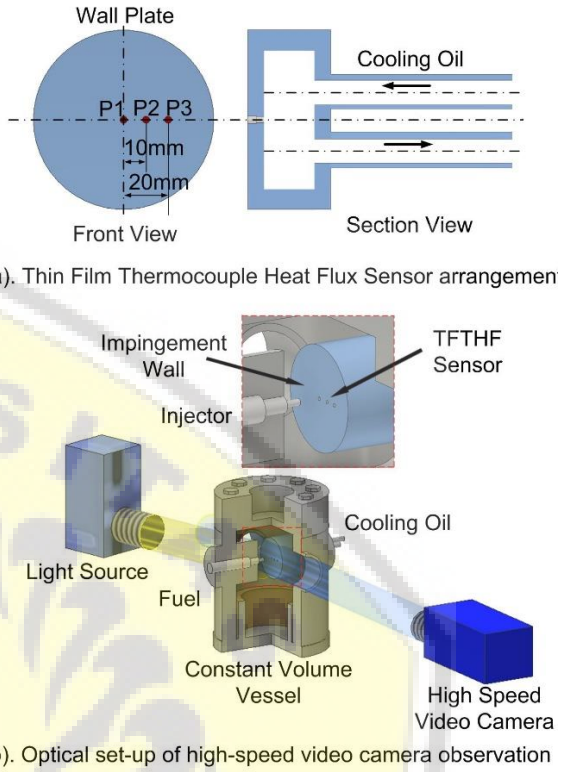

Figure 1. (a) Thin film thermocouple heat flux sensor arrangement and (b) optical set-up of high-speed video camera

For heat transfer correlation, the several empirical correlations to predict the in-cylinder heat transfer coefficient in internal combustion engine (ICE) were reviewed by Finol and Robinson [9]. The most widely used heat transfer correlations were derived by Woschni [10] and Annand [11]. The basis of these correlations has relied on dimensional analysis for turbulent flow that corelates the *Nusselt (Nu)*, *Reynolds (Re)*, and *Prandtl (Pr) numbers*. The relationship among *Nu, Re, and Pr numbers*, which follow those found applied in a turbulent heat transfer equation of the pipe's internal flow or over flat plates [12,13].

Recently, Kuboyama [14] provided alternative correlations that are applicable to recent diesel engines. As characteristic velocity, mean piston speed is typically used in previously proposed heat transfer equations. Kuboyama used flow induced by fuel injection during the fuel injection period for characteristic velocity. After the fuel injection, character velocity was used in Woschni's equation.

$$Nu = (Const)\ x\ Re^m x\ Pr^n \quad (2)$$

$$Nu = \frac{h.L}{\lambda} \quad (3)$$

$$Re = \frac{\rho.U.L}{\mu} \quad (4)$$

$$Pr = \frac{\mu.cp}{\lambda} \quad (5)$$

Where *Nu*, *Re* and *Pr* are difined as the following equation (3), (4), and (5). *m* and *n* are defined based on the laminar or turbulent heat transfer. *L* is characteristic length, λ is thermal conductivity, ρ is density, *U* is characteristic velocity at each position, μ is viscosity and *cp* is specific heat. We used distance between the nozzle tip and the wall as the characteristic length.

Test Conditions

To understand the effects of the injection rate profile, we conducted a non-evaporating spray and combusting spray test to investigate the relation between the spray flame development and heat flux. The experimental condition was summarized in Table 1. To keep the gas density the same for all conditions, i.e. 17.8 kg/m^3, for non-evaporation, ambient pressure was set at 1.5 MPa and for combustion at 4 MPa.

Measurement conditions were determined based on actual operation of small size diesel engines. Pressure and temperature were set at those of compression TDC in low load operation for the combustion test in order that self-ignition of the fuel would be maintained. The impinging distance between the nozzle tip to the wall was set at 40 mm. The injection condition was conducted at three injection pressures, i.e. 58, 68, and 171 MPa using a nozzle of 0.133, 0.122, and 0.101 mm hole size diameter.

Table 1. Experimental conditions.

	Non-Evaporation	Combustion
Fuel		
Fuel	Diesel fuel	←
Ambient Condition		
Ambient gas	N_2	Air (N_2:79%,O_2:21%)
Ambient pressure (MPa)	1.5	4
Ambient temperature (K)	293	780
Ambient density (kg/m³)	17.8	←
Injector and Injection Condition		
Injector type	Piezo actuator type	←
Number of nozzle holes	1	←
Nozzle hole diameter/Injection pressure		
"D_{hole}/P_{inj}" (mm)	0.133/58, 0.122/68, 0.101/171	←
Injection quantity (mm³)	5	←
Impingement Wall		
Impingement wall	Flat plate, Stainless steel	←
Impingement distance "D_{imp}" (mm)	40	←
Wall temperature (K)	293	460 ±10
Coolant method	-	Oil Cooling

RESULTS AND DISCUSSION

Injection Rate Profiles

In order to maintain the similar injection profile, three nozzle hole size diameter were adjusted by different the pressures. The injection rate profile used in this study, which was decided the Nozzle hole diameter and injection pressures (D_{hole}/P_{inj}) 0.133/58, 0.122/68, and 0.101/171 mm/MPa, as shown in Figure 2. It was averaged result of ten times injection rate measurement.

From the graph we can see that similar injection profile was achieved for all conditions. In all conditions were performed as 1.4 ms of injection period, 5 mm^3/ms peak injection rate, and 5 mm^3 of the total fuel injected quantity, respectively.

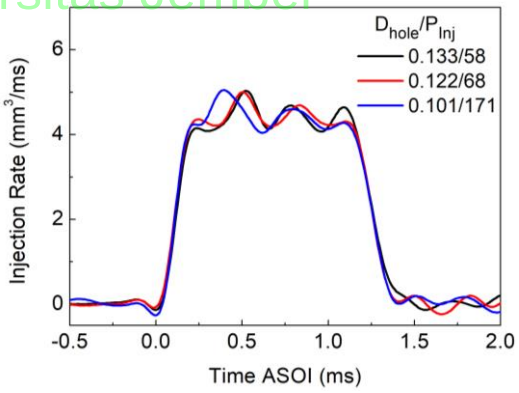

Figure 2. Different nozzle holes diameter at similar injection rate profiles

Development of Non-Evaporating Spray and Spray Flame

In this section, the impinging spray behavior under non-evaporation condition at similar injection profiles were studied. Figure 3. shows line-of-sight images from high speed video camera. The horizontal axis shows time after start of injection (ASOI). Time 0.5 ms to 1.5 ms ASOI represents the spray evolution. Spray can be seen traveling from top to the bottom in each photo and impinging on the wall.

From the spray images, we can see that the development of spray is very similar at all conditions of D_{hole}/P_{inj} 0.133/58, 0.122/68, and 0.101/171 mm/MPa. In all conditions, it follows that the time of spray just before or after impingement on the wall has similar timing at 0.5 ms and 0.9 ms ASOI, respectively. Furthermore, under similar injection rate profiles, it shows a similar shape of spray flows radially spread to circumferential wall area after its impingement to the wall. From these results, it was confirmed that injection rate profile greatly affected the spray development.

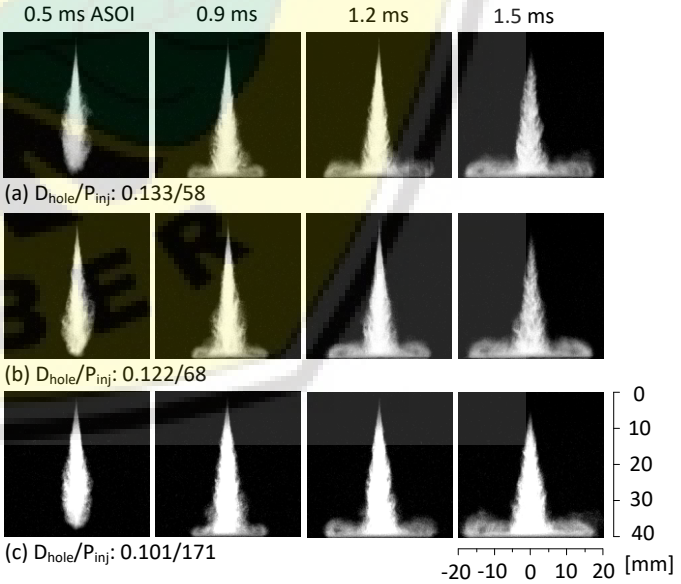

Figure 3. Non-evaporating wall impinging spray at similar injection rate profiles

Figure 4 shows temporal changes of spray tip penetration in vertical axis on the left-side graph and flame length plot in vertical axis on the right-side graph, respectively. Spray tip lengths, which is defined as a summation of axial and radial penetration distances, under similar injection rate profiles obtained from the non-evaporating images. Filled and open markers show before and after the spray impingement on the wall, respectively.

As non-evaporating images, the penetration pattern under similar injection rate profile is also similar in respect of before or after impingement on the wall regardless nozzle hole size diameter and injection pressures. After start of fuel injection in Figure 4, we can see that the spray tip penetration continues to increase even after exceeding the injection duration. Regarding the spray tip penetration being almost similar to each other, it means the spray droplet velocity shows no change and has same fuel momentum.

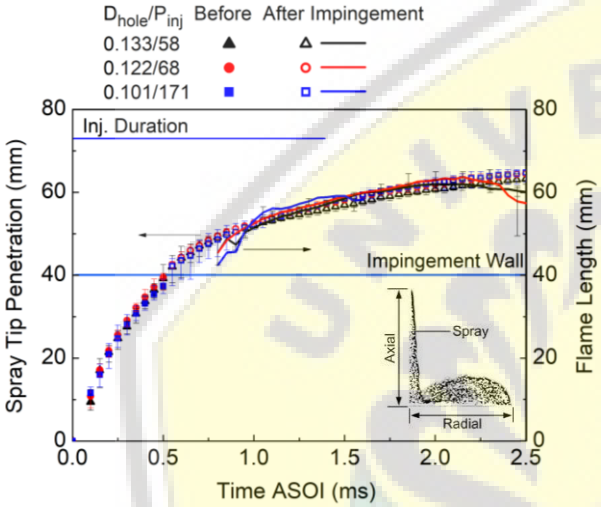

Figure 4. Spray tip penetration and flame length at similar injection rate profiles

Figure 4. in vertical axis on the right-side graph shows flame length histories, as measured using averaged images was obtained from flame luminosity as shown in Figure 5 which will be discussed in the next section. The lengths, which was defined similar to the non-evaporating spray. The flame length starts to increase after spray impingement on the wall at all conditions. Under the similar injection rate profiles, the flame length almost has same trend line due to its similar spray tip penetration. Comparing the flame length with spray tip penetration, it shows a clear trend that has consistently indicate similarity in both length geometry measurement.

Flame Temperature and KL Factor

The effect of similar injection rate profile on combustion process, flame temperature and KL factor were studied. In diesel combustion, radiated luminosity of flame, which is generated from the soot combustion, can represent combustion temperature by black-body radiation theory. Since the natural luminosity mainly comes from soot incandescence in diesel flame, then we analyzed the natural flame images with two-color pyrometry. KL Factor is a measure of soot particulate concentration, where K is the absorption coefficient, nearly proportional to the number density of soot particles, L is the path length of the flame in the direction of the light axis of the flame detection.

Figure 5 shows the luminous flames from the high-speed video color camera. At 0.9 ms ASOI, flame natural luminosity was observed near wall surface area at all varying nozzle hole diameter and injection pressure conditions. At this timing, the ignition delay presence can be detected from these photographs by the luminosity change due to start of a chemical reaction of combustion. It was confirmed that the ignition delay at all conditions became similar. It may be the case that spray mixture was improved by impingement and the combustion occurred after impingement to the wall in all conditions.

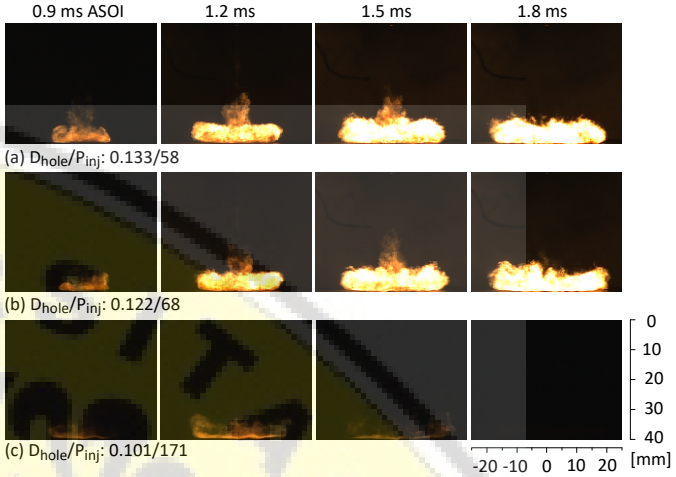

Figure 5. Flame natural luminosity at similar injection rate profiles

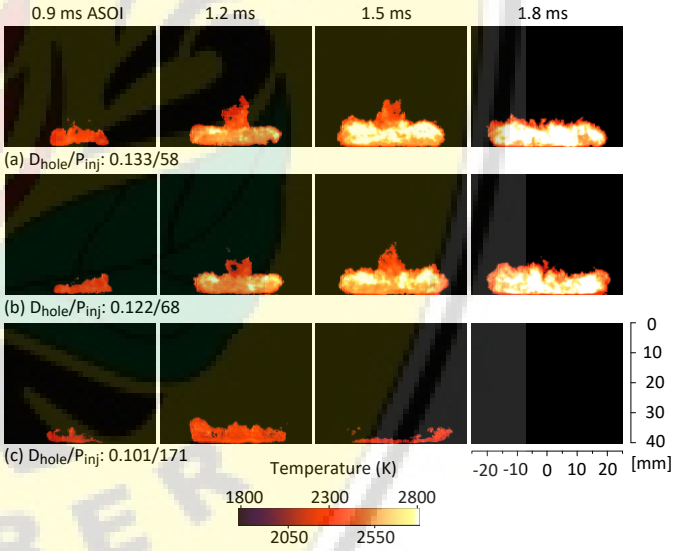

Figure 6. Flame temperature distribution at similar injection rate profiles

The combustion behaviors were similar at all conditions, where the flame spreading with apparent luminosity along the wall after impingement. However, its differed in case flame luminosity intensity only at condition D_{hole}/P_{inj}: 0.101/171 as shown in Figure. 5 (c). In this condition, the effect of smaller nozzle hole diameter and higher injection pressure as shown in Figure 5. (c) which led to further decrease in luminosity intensity compared with the case of larger nozzle hole diameter and lower injection pressure as can be seen in Figure 5. (a-b). This combined effect of nozzle hole diameter and injection pressure on luminosity intensity had been described in the previous report [15]. These phenomena indicate that the effect of

decreasing nozzle hole diameter and increasing injection pressure is an effective way to promote greater premixing between fuel and air during ignition delay, which is more air entrainment with improving spray atomization. Consequently, this leads to premixed combustion, which results in reduced luminosity and shorter combustion duration.

For the heat transfer analysis, information on the temperature distribution of the impinging spray flame is necessary to investigate. Figure 6 shows the flame temperature distributions at similar injection rate profiles using two-color method analysis, which was obtained from natural luminosity of flame. The color distribution scale is varied from dark to bright indicating temperature.

By comparing the temperature distributions under similar injection rate profiles, it showed that the D_{hole}/P_{inj}: 0.133/58 and 0.122/68 had similar shape temperature distribution and they were of higher magnitude of temperature than D_{hole}/P_{inj}: 0.101/171. The shapes of the temperature distribution were identical to those of flame because they were obtained from the flame luminosity. As luminosity diminishing in condition D_{hole}/P_{inj}: 0.101/171 when timing 1.8 ms ASOI as shown in Figure 5 (c), the temperature distribution could not be obtained from non-luminous areas.

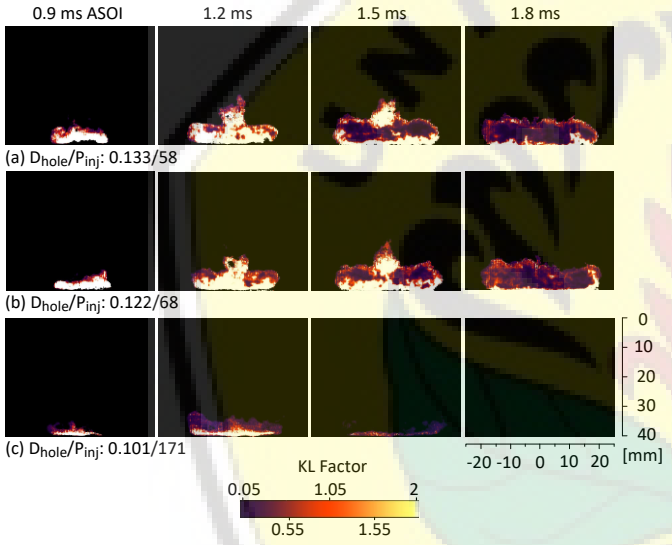

Figure 7. KL Factor distribution at similar injection rate profiles

Figure 7 shows KL Factor distribution under similar injection rate profiles. KL Factor was obtained from images of luminous flame by soot combustion. In the KL factor images, the large soot concentration was detected along the wall surface at all conditions where the flame temperature is lower. These regions indicate that the fuel film could not be avoided under impinging flame condition and high particle concentration is produced whereby combustion was incomplete and rich local equivalence ratio occured along wall surface area.

Comparing the KL Factor distributions under similar injection rate profiles, it presents that the effect small nozzle hole diameter and high injection pressure of D_{hole}/P_{inj}: 0.101/171 produces lower KL Factor value than large nozzle hole diameter and high injection pressure of D_{hole}/P_{inj}: 0.133/58 and 0.122/68.

Figure 8. (a) and (b) shows temporal change of mean temperature and integrated KL Factor each under similar injection rate profiles. From the figures, we can see that there is a significant difference between both D_{hole}/P_{inj}: 0.133/58 and 0.122/68 which have higher value in mean temperature and Integrated KL Factor comparing with the condition of D_{hole}/P_{inj}: 0.101/171. Higher flame temperatures therefore can be explained as follows. At larger nozzle hole diameter and lower injection pressure at both conditions of D_{hole}/P_{inj}: 0.133/58 and 0.122/68, more flame natural luminosity was observed as shown in Figure 5, which was related to temperature and soot volume fractions. In this condition, soot is dramatically higher, which is contributed by less air entrainment with decrease in spray atomization and fuel air-mixing and therefore bringing it to local high equivalent ratio. The correlation of high temperature with local high equivalent ratio is commonly discussed as being accounted for soot production. Instead, natural flame intensity for smaller nozzle hole diameter and higher injection pressure of D_{hole}/P_{inj}: 0.101/171 was reduced. This parameter leads to more air entrainment with improving spray atomization and premixing between fuel and air as results soot formation was reduce.

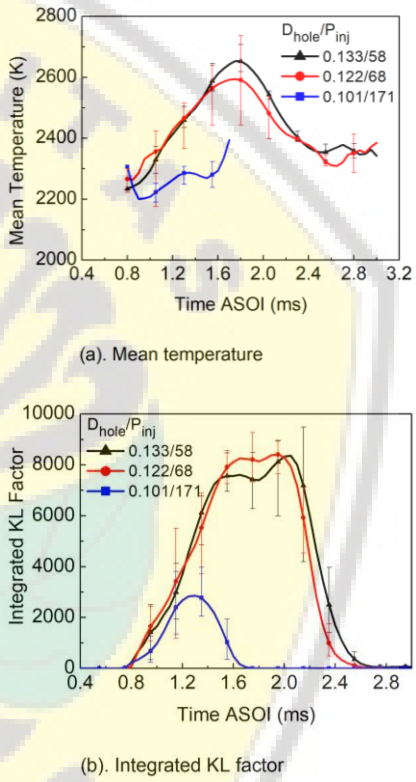

Figure 8. Luminous flame area, mean temperature distribution and Integrated KL Factor at similar injection rate profiles

Spatial distribution of local temperature in near wall under flame impinging becomes important to clarify the heat losses on the wall. Temperature near the wall strongly affects the wall temperature due to rapid heat transfer by convection. Figure 9. shows the areal averaged temperatures at 0.9 mm from wall surface in three areas under similar injection rate profiles. These results in all graphs were obtained from Figure 6.

The graph shows that temperature distribution is varies in the radial direction in time period. It implies strong combustion gas turbulent flow exists together with the combustion reaction especially at Position1 and Position2. Similar as temperature distribution as shown in Figure 6, the local temperature value and resident time decreases

further with smaller hole diameter and higher injection pressure under condition of D_{hole}/P_{inj}: 0.101/171 at all Positions comparing with other conditions.

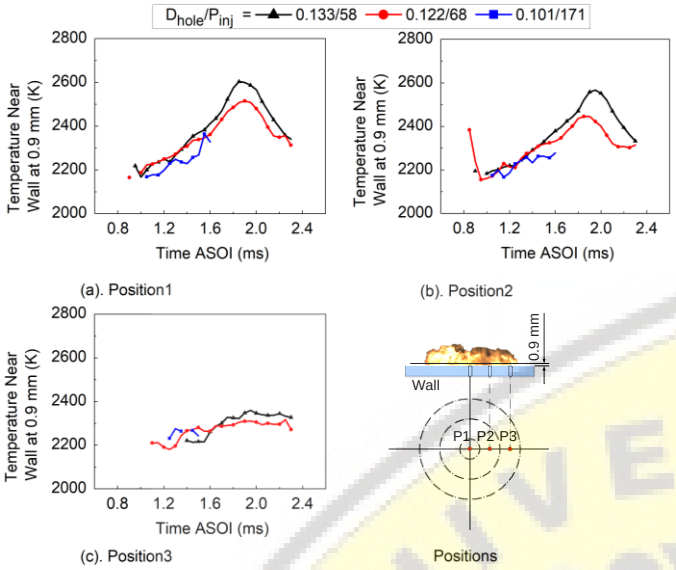

Figure 9. Temperature distribution near wall at 0.9 mm

Comparing among three Positions, temperature decreases along the measurement location from Position1 to 3, due to wall friction and momentum exchange with surrounding gas. Meanwhile, under injection rate profiles, local temperature near wall was slightly lower comparing that mean temperature in Figure 8 (a), as an effect of wall temperature different with flame or ambient surrounding gas.

Wall Heat Transfer

Figure 10. shows unsteady temporal variation of local heat flux and total heat flux of flame impingement on the wall under similar injection rate profiles. Spray impinging and ignition timing were also plotted on the graph. Time histories of local heat fluxes were different at three measurement locations such as Positions1, 2, and 3. These variations can be due to spatial spray and flame flow non-uniformity, leading to heat flux fluctuation.

Spray flame flows radially after impingement on the wall and arrives at different timing each position. Local heat flux at Position1 started to increase after spray impingement on the wall at all conditions. The observed increase in local heat flux at Position1 could be interpreted as being as a result of the effect of convection when a turbulent of evaporating spray impinges to the wall as mentioned in the previous report [15]. Then, combustion gas velocity was mainly responsible for start of the local heat flux peak at Position2. Because the flame spreads to the circumferential area of the wall takes time to reach Position3, the local heat flux at Position3 started to increase later, reaching a value of significantly lower than theothers since both wall friction and momentum loss due to turbulent mixing took place.

The effect of similar injection rate profiles on local heat flux was found significant only at smaller nozzle hole diameter and higher injection pressure of D_{hole}/P_{inj}: 0.101/171. In this condition, a higher peak value of the local heat flux was detected at all positions. A possible explanation for this, smaller nozzle hole diameter and higher injection pressure may be the case that more air entrainment with improving spray atomization thus, premixing between fuel and air due to combustion reaction occurs faster as well as increase in flame velocity. It is evident from the that heat flux value is increased in Position2 rapidly, following the increase in Position1. These increasing flame velocities were toward the wider wall area is also responsible for increased local heat flux at Position3.

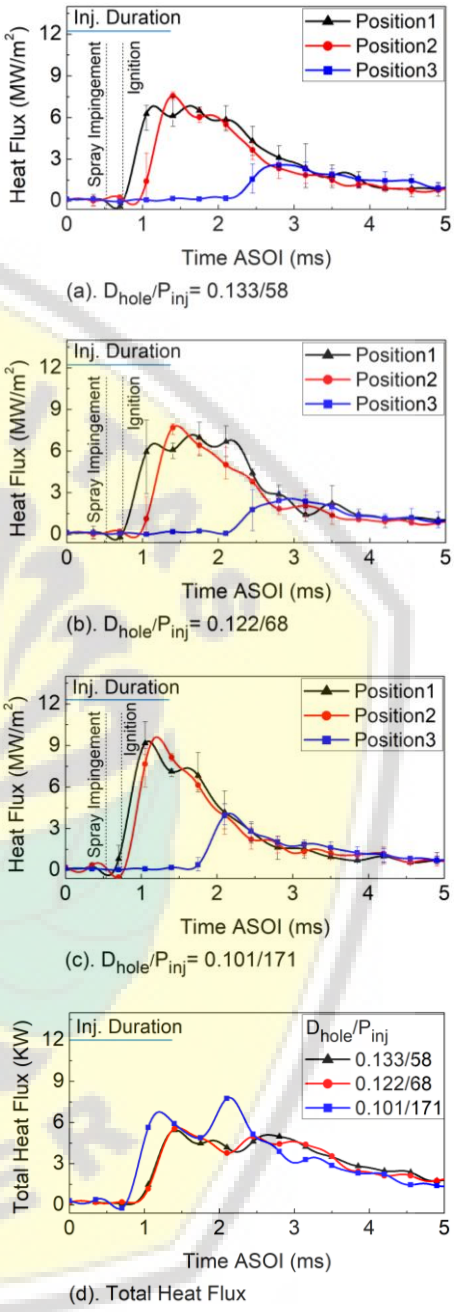

Figure 10. Temporal variation of local heat flux and total heat flux at similar injection rate profiles

The total heat flux under similar injection rate profiles as shown in Figure 10 (d). As we can see from the graph, all of waveforms have two peaks, which means there are two stages for total heat flux. At first, the total heat flux was increased by turbulence of impingement spray and combustion which starts after impingement, and thereafter when the flame contact the wall, it develops to a circular area where

the flame velocity decreases due to the fact that effects of wall friction takes place, then heat transfer occurs.

The effect the total heat flux on similar injection rate profiles shows that the D_{hole}/P_{inj}: 0.101/171 has the maximum temporal variations of total heat flux value compared with other conditions. The area is influential factor for the temporal variations of total heat flux. It was more affected by a smaller nozzle hole diameter and higher injection pressure. This was evident by local heat flux at Positions1, 2, and 3 each has a maximum peak value as shown in Figure 10 (c) compared with larger nozzle hole diameter and lower injection pressure of D_{hole}/P_{inj}: 0.133/58 and 0.122/68 in Figure 10 (a) and (b) respectively.

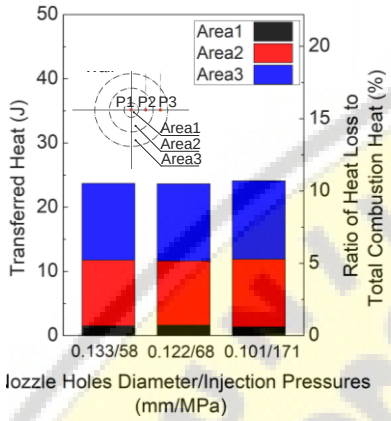

Figure 11. The areal transferred heat and ratio of heat loss to total combustion heat at different similar injection rate profiles

Results of the investigation into transferred heat and ratio of heat loss to total combustion heat under similar injection rate profiles are shown in Figure 11. Transferred heat values are a summation of heat fluxes at the toroidal area of the sensors during the heating period. Vertical axis on the left and right-side of the graph show transferred heat and ratio of heat loss to total combustion heat, respectively.

There were no significant differences between all conditions in terms of transferred heat. This was probably due to similar injection rate profiles. Regarding these results, injection rate profile was an effective strategy for controlling in transferred heat through the wall. It was around 24 Joule of the transferred heat through the wall under similar injection rate profiles and the ratio of heat loss to the wall was about 11% of total combustion energy.

Heat Transfer Coefficient and Nusselt-Reynolds Number Analysis

Heat transfer coefficient and Nusselt-Reynolds number under similar injection rate profiles were observed in this section. The temporal change of local heat transfer coefficients, which were calculated by equation (1) with the measured heat flux during the combustion conditions under similar injection rate profiles, are shown in Figure 12. Therefore, the heat transfer coefficient has similar waveform with local heat flux at all of positions and conditions. As for gas temperature used in the convective heat transfer, an equation was obtained from temperature near wall based on two-color method analysis. It was decided to use the gas temperature near the wall for this study, besides being close to the measurement location with taking into account the importance of the temperature gradient.

The graphs showed that the heat transfer coefficient had a higher value at location of Position1 and 2 than that of Position3 in all conditions. This means that spray flame flow is mostly developed around the location which is not far from the impingement center. Even though injection rate profiles were similar, however, smaller nozzle hole diameter and higher injection pressure lead to higher heat transfer coefficient at all positions. Strong spray flame flow was evident under such conditions. It means that combining the smaller nozzle hole diameter with higher injection pressure, which increases spray flame flow, is one of the most influencing factors for heat transfer coefficient. In this condition, it is evident that result in greater local heat flux value as shown in Figures 10.

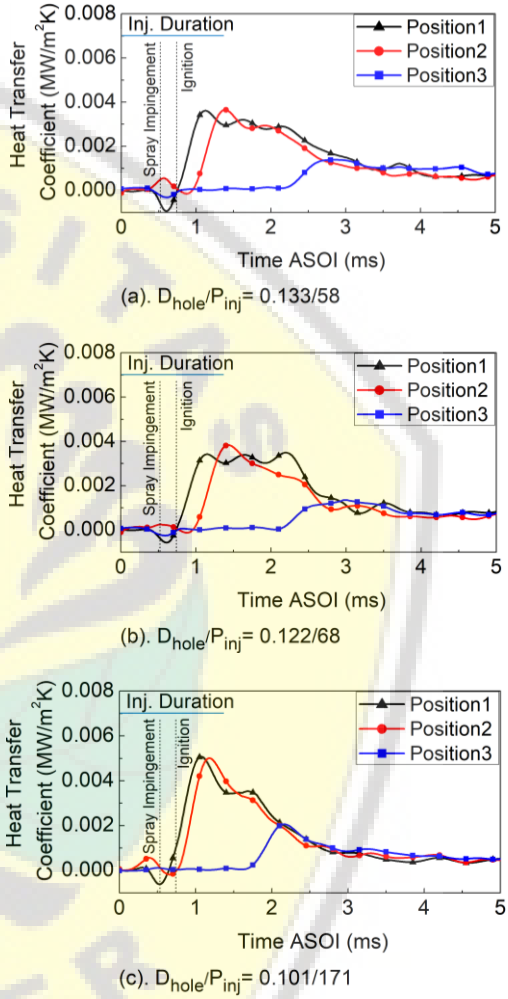

Figure 12. Temporal variation of local heat transfer coefficient at similar injection rate profiles

The spray flame flow has considerable effect on heat loss through the wall, according to the above explanations, Then, we studied relation between *Re number* and *Nu number*. As mentioned in equation (4), *Re number* requires characteristic flow velocity.

As mentioned with Kuboyama, et al. [14], they have provided alternative correlations which are applicable to recent diesel engines. They used flow induced by fuel injection during the fuel injection period for characteristic velocity. After the fuel injection is fully completed, piston speed as characteristic velocity used in the Woshni's equation.

However, it was not possible to estimate the velocity by commonly used measurements, so we utilized waveforms of the heat flux as represented by characteristics velocity. As characteristics velocity, mean piston speed is usually used in previously proposed heat transfer equations.

The waveforms of the heat flux can be seen clearly here, which seems to be as a fact of combustion flame motion. If the peaks were similar in the different positions, by comparing peak by peak we could obtain flamelet velocities along the wall as will be explained in the form of flamelet velocity. The characteristic velocity for the *Reynolds number* obtained from the single-shot heat flux waveform. In order to investigate characteristic flow velocity, flamelet velocity determined according to the local combustion flame motion near wall which has direct impact on local heat flux waveform characteristic. It was assumed that the waveform had clearly identifiable peaks as a consequence of which combustion flame motion.

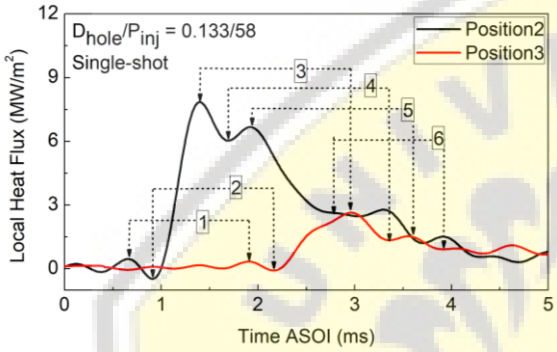

Figure 13. Relation of heat flux wave forms between the two points.

Figure 13. provides a single shot heat flux waveform that shows only Position2 and 3. The method for measuring the flamelet velocity is as follows. First, the distance between Position2 and Position3 was 10 mm, denoted as characteristics length. Position2 and Position3 were chosen with consideration that Positions had a more stable velocity compared to that of Position1, at which it was in a state of stagnation. Next, time value can be detected from measuring the change in waveform between Position2 and Position3 as depicted by number 1 to 6 inside square as shown in Figure 13. According to the time difference between Position2 and Position3 (for example number 1), we obtained time value to calculate characteristic velocity [15].

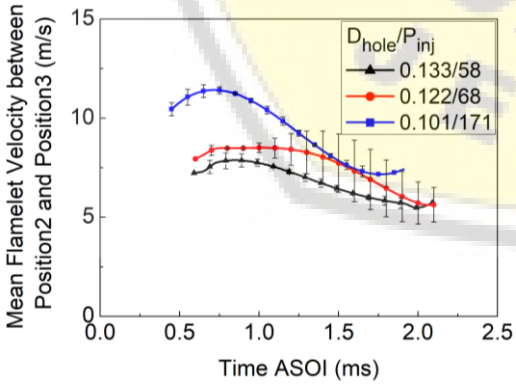

Figure 14. Flamelet velocity at similar injection rate profiles

The results of flamelet velocity measurement at similar injection rate profiles can be seen in Figure 14. Under the effect of similar injection rate profiles, it showed that an increasing nozzle hole diameter and decreasing injection pressure lead to reduce in flamelet velocity. This finding seemed reasonable, as reported by some researches [16,17,18] at which the local flame velocity increased with high injection pressure. Then, we used these values for calculating *Re number*.

The results on correlation between *Reynolds number* and *Nusselt number* under similar injection profiles are presented in Figure 15. Comparison of heat transfer correlation by other researchers were also plotted in graph. For the calculation of the *Re number*, the impingement distance is chosen as a representative length, i.e. 40 mm, whereas those shown in Figure 14 were used for characteristic velocity. For calculation of *Nu number*, thermodynamic properties of air were considered.

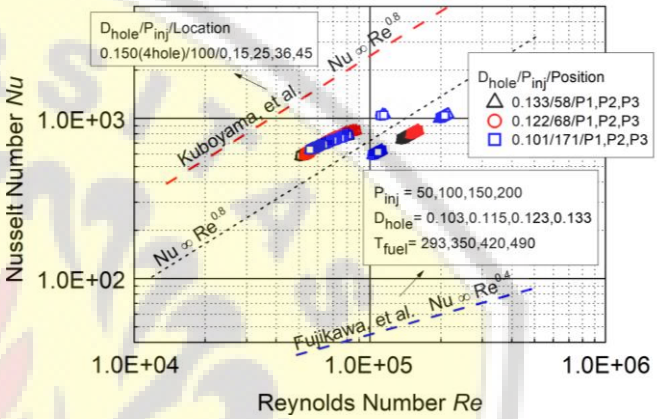

Figure 15. Comparison correlation between *Reynolds number* and *Nusselt number* with other researchers

From the graph in Figure 15 we can see that under similar injection rate profile, the position of points data is in the turbulent flow region. The points show in group and divide into two parts due to its different heat transfer coefficient value at each position (Position1 to Position3) which it will affect the *Nusselt number* value.

It can be seen from the figure the relation between *Nu number and Re number* approximates one line at all of conditions. It was found that *Nu number* was directly proportional to power of 0.8 *Re number* for the combined case. High turbulence flow from combustion which is characterized by high *Reynolds number* is one of the major factors causing a large amount of heat transfer on the wall. Regarding these results, using flamelet velocity to calculate *Re number* was well expressed by this correlation.

Comparing heat transfer correlation of *Reynolds* and *Nusselt number* with other researchers can be explained as follows: in case of characteristics velocity, Kuboyama et al., [14] using flow induced by fuel injection and piston speed. On the other hand, Fujikawa et al., [19] using flame tip velocity as characteristics velocity. Therefore, *Nusselt number* was directly proportional to *Reynolds number* at all researcher conditions. As we can see from the figure, the exponent value of *Reynolds number* was to the power of 0.8, similar one with Kuboyama et al. [14]. However, it was to the 0.4 power in Fujikawa, et al.

In case of *Nusselt number*, *Nusselt number* value was reported slightly higher by Kuboyama et al., [14]. It suggests that the Kuboyama et al., using rapid compression expansion machine in which high turbulent flow occurred with high compression ratio. However, *Nusselt number* value was slightly lower at Fujikawa et al., [19] due to different ambient density and lower characteristics length. It was 27.8 kg/m3 ambient density with 35 mm characteristics length. However, the ambient density and characteristics length in this study are 17.8 kg/m3 and 40 mm. As far as we know that the lower ambient density leads to flame spread wider along the wall with increasing flame velocity. This spray flame flow is one of the significant factors on the heat transfer coefficient. If the heat transfer coefficient and characteristics length have higher values, the Nusselt number will be increased significantly as equation 3.

Conclusions

The effects of nozzle hole size and rail pressure at similar injection rate profiles on the combustion wall heat transfer under diesel engine-like conditions were investigated. The main conclusions of this work are summarized as follows.

1. Under similar injection rate profiles, spray development from spray images are very similar each other. It was also confirmed in that spray tip penetration in respect of before or after impingement on the wall regardless nozzle hole size diameter and injection pressures.

2. Comparing the length of spray tip penetration and flame, it shows a same trend line being consistently similar, which was shown at both respective length geometry measurements.

3. Condition of D_{hole}/P_{inj}: 0.133/58 and 0.122/68 have higher value in mean temperature, temperature near the wall, and Integrated KL Factor comparing with the condition of D_{hole}/P_{inj}: 0.101/171. In this condition, more flame natural luminosity was observed which was related to temperature and soot volume fractions.

4. Under similar injection rate profiles on local heat flux and heat transfer coefficient, it was found significant only at smaller nozzle hole diameter and higher injection pressure of D_{hole}/P_{inj}: 0.101/171. It suggests that more air entrainment with improving spray atomization and premixing between fuel and air were produced. As results, rapid reaction of combustion occurred in addition increase in flame velocity.

5. There were no significant differences between all conditions as far as transferred heat is concerned. This was probably due to similar injection rate profiles. Regarding this result, injection rate profile was an effective strategy for controlling the transferred heat through the wall.

6. A new method for determining characteristic velocity (flamelet velocity) to calculate *Re number* has been proposed. By using the value, it was found that Nu number was proportional to the power of 0.8 of *Re number*.

Acknowledgements

We would like to thank Mazda Motor Corporation for their support with measurement in this study and we gratefully acknowledge Mr. Onur Akgol, for his valuable suggestions and discussions.

References

1. Wakisaka, Y. and Azetsu, A., "Effect of Fuel Injection Rate Shaping and Injection Pressure on Intermittent Spray Combustion," SAE Technical Paper 2000-01-2793, 2000, doi:10.4271/2000-01-2793.
2. Wakisaka, Y. and Azetsu, A., "Effects of Fuel Injection Rate Shaping on Combustion and Emission Formation in Intermittent Spray," SAE Technical Paper 2002-01-1159, 2002, doi:10.4271/2002-01-1159.
3. Benajes, J., Molina, S., De Rudder, and K. Rente, T. Influence of injection rate shaping on combustion and emissions for a medium duty diesel engine. J Mech Sci Technol 20, 1436–1448, 2006, doi:10.1007/BF02915967
4. Yang, K., Yasaki, S., Nishida, K., and Ogata, Y., "Injection Strategy to Enhance Mixture Formation and Combustion of Fuel Spray in Diesel Engine," SAE Technical Paper 2018-01-0241, 2018, doi:10.4271/2018-01-0241.
5. Mahmud, R., Kurisu, T., Nishida, K., Ogata, and et al. Experimental study on flat-wall impinging spray flame and its heat flux on wall under diesel engine–like condition: First report—effect of impingement distance. Proceedings of the Institution of Mechanical Engineers, Part D: Journal of Automobile Engineering, 233(8), 2187–2202, 2018, doi:10.1177/0954407018778153
6. Ahn, S., Matsui, Y., Kamimoto, T., and Matsuoka, S., "Measurement of Flame Temperature Distribution in a D.I. Diesel Engine by Means of Image Analysis of Nega-Color Photographs," SAE Technical Paper 810183, 1981, doi:10.4271/810183.
7. Woschni, G. and Huber, K., "The Influence of Soot Deposits on Combustion Chamber Walls on Heat Losses in Diesel Engines," SAE Technical Paper 910297, 1991, doi:10.4271/910297.
8. Mahmud, R., Kurisu, T., Nishida, K., Ogata, and et al. Effects of injection pressure and impingement distance on flat-wall impinging spray flame and its heat flux under diesel engine-like condition. Advances in Mechanical Engineering, 2019. doi:10.1177/1687814019862910
9. Finol, C. A., & Robinson, K. (2006). Thermal modelling of modern engines: A review of empirical correlations to estimate the in-cylinder heat transfer coefficient. Proceedings of the Institution of Mechanical Engineers, Part D: Journal of Automobile Engineering, 220(12), 1765–1781. https://doi.org/10.1243/09544070JAUTO202
10. Woschni, G., "A Universally Applicable Equation for the Instantaneous Heat Transfer Coefficient in the Internal Combustion Engine," SAE Technical Paper 670931, 1967, doi:10.4271/670931.
11. Annand, W. J. D. Heat Transfer in the Cylinders of Reciprocating Internal Combustion Engines. Proceedings of the Institution of Mechanical Engineers, 177(1), 973–996, 1963, doi:10.1243/PIME_PROC_1963_177_069_02
12. J. B. Heywood, Internal Combustion Engine Fundementals, vol. 21. New York: McGraw-Hill, 1988.
13. Chang, J., Güralp, O., Filipi, Z., Assanis, D. and et al., "New Heat Transfer Correlation for an HCCI Engine Derived from Measurements of Instantaneous Surface Heat Flux," SAE Technical Paper 2004-01-2996, 2004, doi:10.4271/2004-01-2996.
14. Kuboyama T, Moriyoshi Y and Kosaka H. Heat transfer analysis in a diesel engine based on a heat flux measurement using a rapid compression and expansion machine. SAE paper 2107-320115, 2017.
15. Mahmud, R., Kurisu, T., Akgol, O., Nishida, K. and et al., "Characteristics of Flat-Wall Impinging Spray Flame and Its Heat

Transfer under Diesel Engine-Like Condition: Effects of Injection Pressure, Nozzle Hole Diameter and Impingement Distance," *SAE Int. J. Adv. & Curr. Prac. in Mobility* 2(1):319-329, 2020, doi:10.4271/2019-01-2183.

16. Li, S., Kamimoto, T., Kobori, S., and Enomoto, Y., "Heat Transfer From Impinging Diesel Flames to the Combustion Chamber Wall," SAE Technical Paper 970896, 1997, doi:10.4271/970896.
17. Tatsumi T, Maeda S, Miyata S, and et al. A study on the wall heat loss in diesel spray flame (First report: effect of injection pressure on the heat flux–20165320). Trans Soc Automot Eng Japan, 47: 1291–1296, 2016. (in Japanese).
18. Zama Y, Odawara Y and Furuhata T. Experimental investigation on velocity inside a diesel spray after impingement on a wall. Fuel, 203: 757–763, 2017, doi:10.1016/j.fuel.2017.04.099
19. S. Fujikawa, M. Nakata, S. Maeda, N. Arai, and et al., "Proposal of Wall Heat Transfer Coefficient Applicable to Spray-wall Interaction Process in Diesel Engines," Trans. Soc. Automot. Eng. Japan, pp. 1120–1125, 2018.

Contact Information

Keiya NISHIDA
Department of Mechanical Systems Engineering,
University of Hiroshima
Telephone: +81-82-424-7557
Email: nishida@hiroshima-u.ac.jp
Address: A3-112, 1-4-1 Kagamiyama, Higashi- Hiroshima, JAPAN